ISSN: 2319-5967
ISO 9001:2008 Certified
International Journal of Engineering Science and Innovative Technology (IJESIT)
Volume 2, Issue 1, January 2013

A Survey on Image Upscaling

Supriya S. Thombre, Dr.L.G.Malik
Department of Computer Science & Engineering
G.H. Raisoni College of Engineering, Nagpur, India

Abstract– Creating an upscaled image from a Low-Resolution (LR) Image is very interesting. The nature and texture of an image should be maintained during the upscaling of an image. This upscaling is also termed as "super-resolution". It is related to both statistical relationships between low-resolution and high resolution (HR). Different algorithms are available for super-resolution of an image.

***Index Terms*- Image Super Resolution, Image Upscaling, Techniques For Image Upscaling, Approaches For Image Upscaling, Algorithms For Image Super Resolution.**

I. INTRODUCTION

Sometimes we need an upscaled image to be represented from an original image. It should acquire a "natural" texture. The quality of an image should be maintained while upscaling an image. It is related to both statistical relationship between LR and HR image sampling and to the human perception of image quality [1][3].

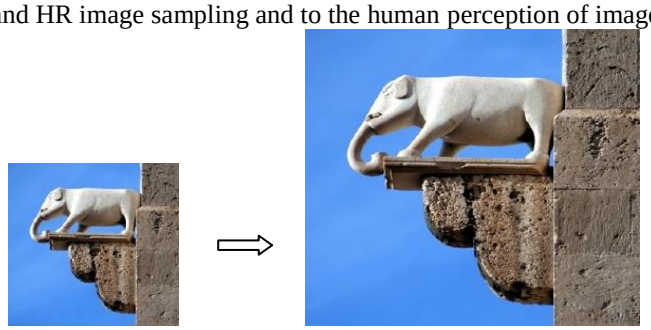

Fig. 1 Example of image upscaling.

Fig.1 gives the example of image up scaling. There are different methods through which the image can be upscaled. Some of the them are viz. polynomial interpolation, statistical methods, and edge-directed interpolation. The polynomial interpolation is a simple method which is based on linear filtering. This method is computationally efficient and on the other hand the images are blurred and jagged contours. The statistical method use pixels statistics or database of example to obtain good high resolution image. It is used to make variety of natural textures and scales. The only disadvantage of this method needs a sufficiently representative set of examples. The edge-directed interpolation tries to improve the accuracy of the interpolation characterizing the edge features in a larger region. They aim at interpolating along edges rather than across them to prevent blurring. This method has good results for natural images. On the other hand they require high computationally. Bilinear or Bicubic interpolation tend to generate overly smooth images consisting ringing and jagged artifacts, interpolation by exploiting the natural image priors will generally produce more favourable results [2]. There are some other ways through which the image up scaling is possible. Section II includes different approaches for super-resolution of an image. We propose some future enhancement in this area in section III. Section IV concludes this paper.

II. APPROACHES FOR SUPER-RESOLUTION OF AN IMAGE

In this section we give brief overview of some of the existing techniques in image up scaling, along with their simulation results. We discuss our view on each of the approach and the future enhancement possible in this particular area.

A. Effective Iterative Back Projection Approach

This technique proposed by Bajera and Modi [4] was based on an Iterative back projection (IBP) method combined with the Canny Edge Detection and error difference image to recover high frequency information. The IBP method can minimize the error significantly by back projecting the error iteratively. It uses simple bicubic interpolation to enlarge the image and processes it according to the IBP method. It also back projects

ISSN: 2319-5967
ISO 9001:2008 Certified
International Journal of Engineering Science and Innovative Technology (IJESIT)
Volume 2, Issue 1, January 2013

high frequency component using Canny Edge Detection and difference images of upsampled LR images to gather more back projecting error.

Algorithm:

The first interpolated image $X^{(0)}$ was obtained by enlarging the original low resolution image y same as the IBP method. $X^{(n)}$ was an estimated high frequency image which was degenerated from an estimation of low resolution image y. So, in the iteration process, the estimated high resolution image $X^{(n)}$ will be the more similar to the original HR image $X^{(0)}$. The HR image X' was interpolated from an estimated low resolution image $y^{(n)}$. It could be predicated that X' will have more serious blurring effect than $X^{(0)}$. The lost high frequency data ($X(0) - X'$) was calculated and back projected to the estimated HR image to compensate the high frequency error for overcoming this effect. The iteration process reduces the blurring effect while preserving edges. Fig. 2 denotes the flowchart for the algorithm [4].

The mathematical formulation for estimated HR image after n iterations is expressed as:

$$X^{(n+1)} = X^{(n)} + X_e^{(n)} - X_H^{(n)} \quad (1)$$

The high frequency estimation is given as

$$X_H^{(n)} = X_H^{(0)} - \{((y)I^2_{BC}) - ((y^{(n)}U_S^2)\} \quad (2)$$

Where $X_H^{(n)}$ is a high frequency component after nth iteration , I^2_{BC} is bicubic interpolation by factor 2.

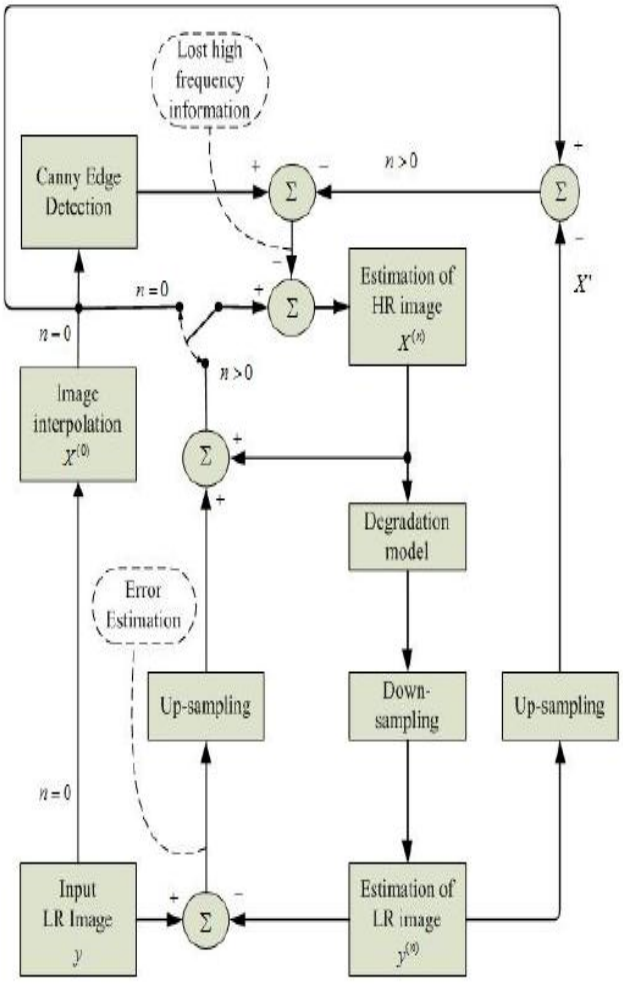

Fig. 2 Flowchart For Algorithm [4].

Several natural gray Images were simulated. In these, initial input LR image was generated from original HR image and apply different algorithms including nearest neighbour (NN) interpolation, bilinear (BL) interpolation, bicubic (BC) interpolation, previous work IBP with LOG as high pass filter [15], IBP with Edge preserving ISEF [16] and proposed method by them, IBP with Canny edge detection and different image on initial input LR image were used, so that resultant image can compared with original HR image.

ISSN: 2319-5967
ISO 9001:2008 Certified
International Journal of Engineering Science and Innovative Technology (IJESIT)
Volume 2, Issue 1, January 2013

Table I. MSE Comparison [4]

Image No	NN	BL	BC	IBP with LOG	IBP with ISEF	Proposed Algorithm
1	102.8143	92.6318	90.9727	52.3896	56.5302	50.8137
2	290.5738	279.4154	268.0110	207.8366	208.6979	194.8016
3	565.2540	529.5540	482.6502	341.7525	350.6396	322.9333
4	252.3951	225.4258	212.9728	159.9113	163.8207	148.9168
5	240.8464	226.7173	215.6824	154.3898	159.4124	151.8006
6	227.6017	211.7113	205.2112	110.6038	119.2341	108.4708
Average	248.1763	230.0701	219.1999	147.1737	153.1088	140.9452

Table II. MAE Comparison [4]

Image No	NN	BL	BC	IBP with LOG	IBP with ISEF	Proposed Algorithm
1	4.4313	4.4382	4.2541	3.4973	3.6373	3.5080
2	7.4196	7.3496	7.0098	6.3791	6.4158	6.2661
3	14.8148	15.2597	14.1945	11.9904	12.2951	11.8527
4	9.2834	9.2921	8.9489	7.6657	7.8446	7.5673
5	8.6965	8.7356	8.3377	6.8793	7.0546	6.8394
6	6.4549	6.5384	6.1767	5.0893	5.1936	5.0097
Average	8.5167	8.6022	8.1536	6.9168	7.0735	6.8405

Table III. PSNR Comparison [4]

Image No	NN	BL	BC	IBP with LOG	IBP with ISEF	Proposed Algorithm
1	28.0103	28.4632	28.5417	30.9383	30.6079	31.0709
2	23.4982	23.6683	23.8493	24.9536	24.9356	25.2348
3	20.6084	20.8917	21.2945	22.7937	22.6821	26.4013
4	24.1100	24.6008	24.8476	26.0920	25.9871	26.4371
5	24.3134	24.5760	24.37927	26.2446	26.1055	26.3180
6	24.5590	24.8734	25.0088	27.6931	27.3667	27.7776
Average	24.1832	24.5122	24.7224	26.4525	26.2808	26.6403

The image quality was determined by MSE (Mean Square Error), PSNR (Peak Signal to Noise Ratio) and MAE (Mean Absolute Error) evaluation. Table I, table II and table III denotes the MSE, MAE and PSNR comparison [4]. From these, it can be concluded that the proposed algorithm by minimizes MSE & MAE types of errors and

ISSN: 2319-5967
ISO 9001:2008 Certified
International Journal of Engineering Science and Innovative Technology (IJESIT)
Volume 2, Issue 1, January 2013

improves PSNR considerably. Their proposed algorithm provides high value of PSNR and low value of MSE & MAE.

Advantages: Their proposed technique was fast and robust to noise with edge perseveration. After multiple iterations, the blurring effect can be greatly reduced in enlarged images. It also provides sharp edges.

B. Coupled Dictionary Training

This technique proposed by Yang, Wang et al. [5] used novel coupled dictionary training method for single-image SR based on patch wise sparse recovery. The learned couple dictionaries relate the LR and HR image patch spaces via sparse representation. The learning process enforces that the sparse representation of a LR image patch in terms of the LR dictionary. It can well reconstruct its underlying HR image patch with the dictionary in the high-resolution image patch space. The learning problem was modelled as a bi-level optimization problem, where the optimization includes an l^1-norm minimization problem in its constraints. The gradient for stochastic gradient descent was calculated by using implicit differentiation. The coupled dictionary learning method can outperform the existing joint dictionary training method both quantitatively and qualitatively. The algorithm can be speed up approximately 10 times for real applications. It was possible by learning a neural network model for sparse inference.

Sampling a large number of training HR/LR image patch pairs from an external database containing clean HR images $\{Xi\}^{n}_{i=1}$ was used to train the coupled dictionaries. LR image was obtained by blurring and down sampling each HR image Xi. By using "bicubic" interpolation upscale the LR image back to its original size to get the interpolated LR image Yi. From these image pairs $\{Xi , Yi \}^{n}_{i=1}$, N pairs of HR/LR patches of size p×p, was sampled and extract their patch features using the aforementioned procedures for obtaining training data $\{(xi , yi)\}^{N}_{i=1}$. The coupled dictionaries Dx and Dy were learnt from the training data which was prepared by eliminating the patches having small variances for avoiding sampling too many smooth patches that were less informative.

Algorithm

1: **input:** training patch pairs $\{(x_i, y_i)\}_{i=1}^{N}$, and diction size *K*.
2: **initial:** initialize $\boldsymbol{D}x^{(0)}$and $\boldsymbol{D}y^{(0)}$, $n=0$, $t=1$.
3: **repeat**
4: **for** i=1,2,…..N do
5: Compute gradient $\alpha = dL(\boldsymbol{D}x^{(n)}, \boldsymbol{D}y^{(n)}, x^i, y^i)/d$;
6: Update $D_y^{(n)} = D_y^{(n)} - \eta(t) \,.\, \alpha$;
7: Project the columns of $D_y^{(n)}$ onto the unit ball;
8: $t = t + 1$;
9: **end for**
10: Update $D_y^{(n+1)} = D_y^{(n)}$;
11: Update $D_x^{(n+1)}$with $D_y^{(n+1)}$;
12: $n = n + 1$;
13: **until** convergence
14: **output**: coupled dictionaries $D_x^{(n)}$ and $D_y^{(n)}$.

1) *Line 2*: Initialize $\boldsymbol{D}x$ and $\boldsymbol{D}y$ with various methods:

a) Train $\boldsymbol{D}x$ from $\{\boldsymbol{x}i\}^{N}i$=1 using standard sparse coding, or mathematically define it, and initialize $\boldsymbol{D}y$ with a random matrix;

b) Initialize $\boldsymbol{D}x$ and $\boldsymbol{D}y$ with those trained from joint sparse coding.

2) *Line 6*: $\eta(t)$ was the step size for stochastic gradient descent, which shrinks in the rate of $1/t$.

3) *Line 7*: To satisfy the dictionary norm constraint, normalize each column of $\boldsymbol{D}y$ to unit l^2-norm.

Advantages: This coupled learning algorithm was generic, and hence can be potentially applied to many signal recovery and computer vision tasks, e.g., image compression, texture transfer, SR etc.

C. Sparse Neighbor Embedding(NE)

This technique suggested by Gao, Zhang et al. [6] used a sparse neighbor selection scheme for SR reconstruction. First predetermine a larger number of neighbors as potential candidates and develop an extended Robust-SL0 algorithm to simultaneously find the neighbors and to solve the reconstruction weights. They suggested that the k-nearest neighbor should have similar local geometric structures based on clustering. For performing such clustering, it employs histograms of oriented gradients (HoG) of LR image patches. The NE-based SR algorithms can represent more patterns even if a relatively smaller training data set was available and thus show much stronger generalization ability for a variety of images.

ISSN: 2319-5967
ISO 9001:2008 Certified
International Journal of Engineering Science and Innovative Technology (IJESIT)
Volume 2, Issue 1, January 2013

Algorithm

1: The LR image I_l *and the size of LR patch s x s;*
2: The neighborhood size *k* and an integer *K;*
3: The HoG centroid set G = $\{\bar{g}^{©}\}^{C}_{c=1}$ obtained by K-means clustering;
4: The training data set
5: $X_s = U^{C}_{c=1} X_s^{©}$ and $Y_s = U^{C}_{c=1} Y_s^{©}$

Table IV. Result of Reconstructed Image using Different Methods [6]

Image No	BI	NE-Based SR	NeedFS	SC-Based SR	TV-Based	ASDS	Proposed Algorithm (BI Interpolation)
1	22.09	23.28	21.55	24.13	25.63	27.09	27.08
	0.773	0.83	0.811	0.866	0.884	0.898	0.903
	0.784	0.831	0.823	0.844	0.846	0.872	0.884
2	26.48	27.38	25.89	27.41	27.73	29.97	29.48
	0.846	0.872	0.846	0.887	0.885	0.909	0.906
	0.905	0.906	0.884	0.918	0.921	0.941	0.944
3	21.82	22.70	21.84	23.18	23.13	24.48	24.34
	0.631	0.728	0.715	0.754	0.762	0.794	0.784
	0.774	0.802	0.797	0.829	0.825	0.851	0.849
4	26.22	26.47	25.73	27.11	27.37	29.19	28.76
	0.73	0.791	0.781	0.812	0.825	0.848	0.838
	0.822	0.827	0.824	0.867	0.848	0.890	0.881
5	31.67	31.55	30.08	31.72	31.57	33.54	33.07
	0.767	0.788	0.775	0.801	0.807	0.824	0.817
	0.871	0.878	0.869	0895	0.882	0.918	0.906
6	28.27	29.05	27.95	29.20	29.14	30.92	30.97
	0.809	0.85	0.834	0.854	0.856	0.871	0.873
	0.839	0.863	0.85	0.881	0.88	0.900	0.895
7	21.85	22.31	20.94	23.26	23.81	26.72	25.99
	0.734	0.832	0.802	0.855	0.877	0.905	0.892
	0.775	0.825	0.836	0.843	0.858	0.877	0.883
8	29.72	30.51	28.64	31.41	31.34	33.47	32.69
	0.829	0.865	0.851	0.883	0.885	0.909	0.902
	0.878	0.89	0.874	0.901	0.91	0.928	0.919
Average	26.01	26.66	25.33	27.18	27.46	29.42	29.05
	0.765	0.820	0.802	0.839	0.848	0.870	0.864
	0.831	0.853	0.845	0.872	0.871	0.897	0.895

In Table IV [6] different algorithms were compared in terms of PSNR (Peak Signal to Noise Ratio), SSIM (Structural Similarity), & FSIM (Feature Similarity). The main advantage of NE algorithm was that the model was simple and easy to implement. On the contrary, the ASDS method was more complex because of the sparse prior regularization, the non-local similarity regularization, and the local smooth regularization was simultaneously incorporated for the SR problem. The proposed method produces top-level visual quality.

D. Multisurface Fitting

This technique proposed by Zhou, Yang and Liao [7] used a new interpolation-based method of image super-resolution reconstruction. The LR pixels were fitted with one surface and the HR images were obtained by fusing multisampling values of these surfaces in *a posteriori* fashion. They recommended that more LR pixels can effectively contribute to the final estimations through their surfaces.

Advantages: *First,* it outperforms other interpolation- based approaches with respect to preserving image details, e.g., higher order information can be preserved. *Second,* unlike the iterative techniques using regularization, it does not need any artificial hypothesis on image prior.

ISSN: 2319-5967
ISO 9001:2008 Certified
International Journal of Engineering Science and Innovative Technology (IJESIT)
Volume 2, Issue 1, January 2013

Algorithm

The intensity of the HR pixel was denoted by p_H which was to be estimated. In the neighbourhood of p_H, there were different LR pixels denoted by (p_{L1} ….. p_{Li}….. p_{LK}), where *K* was the number of LR pixels in the neighbourhood of p_H. A surface was fitted with local smoothness from a group of LR pixels (p_{L1} ….. p_{Li}….. p_{LK}). The fitted surface can be regarded as the continuous image. The HR pixel p_H was obtained by resampling the surface. This process was formulated as

$$\Gamma = \Gamma\ (f(p_{L1}) \ldots f(p_{Li}) \ldots\ldots f(p_{LK}), x_{L1} \ldots x_{Li} \ldots x_{LK}, y_{L1} \ldots y_{Li} \ldots y_{LK}) \quad (3)$$

$$f(p_H) = S\ (x_H, y_H, \Gamma) \quad (4)$$

Γ denotes the fitted surface for multipixels, $f(p_\phi)$ denotes the intensity of pixel p_ϕ. x_ϕ *and* y_ϕ represents the location of pixel p_ϕ in abscissas and ordinates of HR grid respectively. $S(x_\phi, y_\phi, \Gamma)$ was an operation of sampling the surface Γ at location (x_ϕ, y_ϕ). $\phi \in \{HL1 \ldots Li \ldots LK\}$.

They concluded that the spatial structures in the HR grid should comprise two aspects. *One* was the spatial distributions of LR pixels in the HR grid. *Second* was the local structures of intensity, i.e., edge orientations, curvatures, etc. The first aspect was represented by the positions of LR pixels in the coordinate system of the HR grid, and the second was denoted by intensity derivatives of different orders.

Fit one surface at each site of LR pixels by considering the difference of LR pixels. There was a one-to-one correspondence between fitted surfaces and LR pixels. Then, a series of intensity values was obtained at the location of pixel p_ϕ by sampling all *K* surfaces.

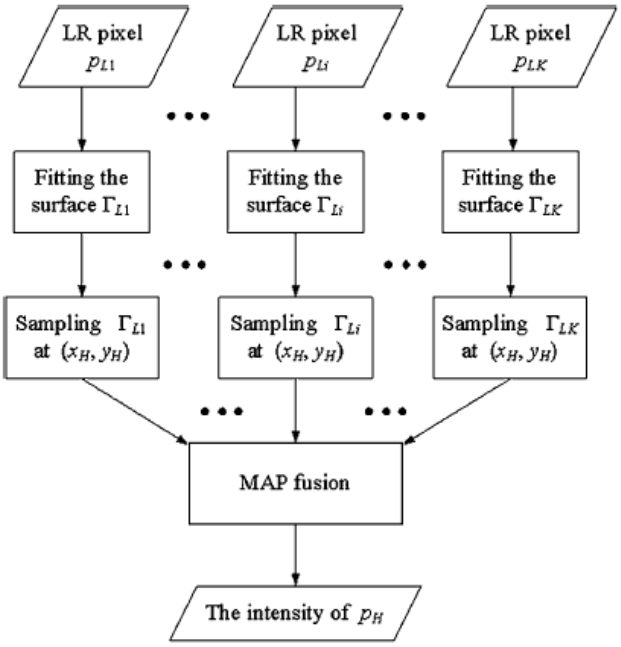

Fig. 3 Flowchart Of Algorithm.

E. Joint Learning via a Coupled Constraint

This technique suggested by Gao, Zhang et al. [8] mainly contains three parts. *First*, preprocessing was used to construct k-nearest grouping patch pairs (GPPs) by linking the LR and its corresponding HR features together. In the *second* step, joint learning was performed to learn two projection matrices of the nearest GPPs associated with each LR input patch such that the difference between LR and HR was reduced as much as possible. Thereafter, the measurements of LR and HR features in the corresponding GPPs were projected onto a unified feature subspace. Then, the NE algorithm was used to estimate the optimal weights in the learned unified feature subspace and combine linearly the corresponding high-frequency patches with the estimated weights to synthesize the HR image patches. *Finally*, back projection was incorporated into the maximum *a posteriori* (MAP) framework, where the global construction constraint and the prior knowledge (that the final output of the HR image should be as close as possible to the initial SR estimate) were combined to enhance the initial SR image.

Algorithm

1: Training data sets $Xs = \{x^i_s\}^N_{i=1}$, $Ys = \{y^i_s\}^N_{i=1}$ and $Zs = \{z^i_s\}^N_{i=1}$;

ISSN: 2319-5967
ISO 9001:2008 Certified
International Journal of Engineering Science and Innovative Technology (IJESIT)
Volume 2, Issue 1, January 2013

2: GPPs *set* $\{G^i\}^N_{i=1}$; LR image *Y*;
3: The size of LR image patch *qxq*;
4: Neighborhood sixe *k*;
5: Dimension *p* of the unified feature subspace to be projected.

Table V. Result of Reconstructed Image using Different Algorithms in terms of RMSE, PSNR, SSIM

Image No	Methods				
	Bi-cubic	NESR	NeedFS	PSNE	Proposed
1	13.545	11.292	10.926	11.108	9.817
	25.495	27.076	27.326	27.239	28.291
	0.7758	0.7963	0.8036	0.7973	0.8404
2	10.338	9.166	8.922	9.027	8.206
	27.842	28.887	29.122	29.02	29.848
	0.8116	0.8222	0.8317	0.8286	0.8557
3	12.659	11.475	9.812	9.153	8.929
	28.788	26.936	28.296	28.899	29.115
	0.7996	0.7845	0.8358	0.8381	0.8630
4	16.947	15.037	13.957	14.273	13.534
	23.549	24.587	25.235	25.041	25.502
	0.6562	0.6582	0.7028	0.6965	0.7402
5	17.323	16.565	15.907	15.85	14.908
	23.359	23.747	24.099	24.13	24.662
	0.6352	0.6478	0.6670	0.6742	0.7051
6	9.272	8.088	8.244	8.139	6.998
	26.082	29.974	29.808	29.919	31.231
	0.8134	0.8165	0.8023	0.819	0.8623
7	6.024	7.057	7.863	6.588	6.457
	32.534	31.158	30.219	31.755	31.93
	0.7933	0.7876	0.7731	0.7885	0.7912
8	8.027	8.755	12.849	8.71	8.682
	30.039	29.286	25.953	29.33	29.358
	0.8494	0.8558	0.8337	0.8601	0.8677
Average	11.767	10.929	11.06	10.356	9.692
	27.211	27.706	27.512	28.167	28.742
	0.7668	0.7711	0.7813	0.7878	0.8157

In the Table V [8] different algorithms were compared in terms of RMSE (Root Mean Squared Error), PSNR & SSIM for 3 x Scale Factor. The RMSE values of their proposed method on eight test images were smaller than those of NE-related algorithms. The PSNR values show that the proposed method was superior to others. It was partly due to the coupled constrain on the LR & HR image patches as well as the fact that the joint learning was able to probe better matching for the desired HR patches. The NE for SR reconstruction in the unified feature subspace enforces a much stronger constraint which reduced the ambiguity between the LR image patches and the HR patches. The SSIM scores also suggested the effectiveness of their proposed method.

F. Local Consistency Constrained Adaptive Neighbor Embedding

This technique proposed by Fan, Sun et al. [9] used a robust single image SR method for enlarging low quality text image. Firstly the non-local reconstruction problem was pointed out in neighbor embedding based super-resolution by statistical analysis on an empirical data set. Secondly, introduce a local consistency constraint to explicitly regularize the linear reconstruction process, and adaptively generate the most possible candidates for the HR image patch. Rely on the adjacent overlapping patches for capability verification through a Markov network of the non-consistent candidates.

ISSN: 2319-5967
ISO 9001:2008 Certified
International Journal of Engineering Science and Innovative Technology (IJESIT)
Volume 2, Issue 1, January 2013

Algorithm

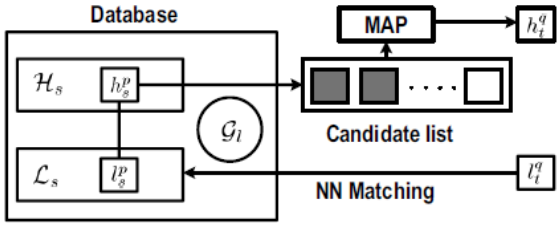

Fig. 4 Algorithm

In the learning phase, large volumes of text primitive patches were extracted from both the LR and HR training images $\mathcal{L}s$ and $\mathcal{H}s$. The LR patches are organized as a local consistency graph $\mathcal{G}_l$. During the synthesis phase, each patch l^t_q from a LR image was presented to the system. A set of adaptively selected HR candidates were retrieved from the training set by nearest neighbor (NN) matching. Each element h^t_q in the target HR image comes from the MAP (*maximum a posterior)* estimation of a Markov network based on the candidate list.

Table VI. RMSE And RMSEB Of Four SR Methods

	Bilinear	Cubic-spline	Proposed method
RMSE	21.7	20.3	12.4
RMSEB	35.4	32.2	23.1

In Table VI [9] different algorithms were compared in terms of RMSE (Root Mean Squared Error), RMSEB (Root Mean Squared Error of Binarized images). The table shows the average RMSE errors over 10 test images for different methods.

G. Edge-Preserving using Preconditioning

This technique proposed by Pelletier and Cooperstock [10] increased the priority of LR images' gradient region, learns from other HR images' gradient region, gets horizontal and vertical direction of image gradient map and links the two gradient maps to get the super-resolution image. The shift matrices were determined by the relative displacements between LR frames. The image was blurred using a 5x5 Gaussian kernel. It was then down sampled. Construction & updation of the preconditioned was used after every iteration.

H. Gradient Learning

Based on the traditional magnification methods that learn through training sets, the method proposed by Li and Peng [11] increases the priority of low-frequency images' gradient region and learns from gradient region. Features were extracted from every gradient image fragment, and then find the closest matching fragments to determine the high-frequency of target image. At first, horizontal and vertical gradient images of the input image was obtained then the two images were combined together to get the final HR image. By this way, the target image had sharper edges and higher quality. It was a very flexible technique.

I. Averaged Image and Regularized Deconvolution

In this technique suggested by Park [12], the LR images were down sampled by shifting the original image by sub-pixel distances which was an average light intensity on the corresponding pixel area. The average of multiple LR images with appropriate registration can be considered as a blurred HR image which was based on down sampling. The HR image was obtained by regularizing the deconvoltion method after identifying the point spread function (PSF). The regularization factor was determined by line search of a cost function.

J. Nonparametric Bayesian INLA Approximation

It was a fully automatic SR algorithm which used a nonparametric Bayesian inference method based on numerical integration known in the statistical literature as Integrated Nested Laplace Approximation (INLA) [13]. It uses a statistical inference in Bayesian frameworks. The INLA only can be applied to latent Gaussian models, where the covariance matrix was governed by a few parameters and the latent field was a Gaussian Markov random field (GMRF) with a sparse precision matrix. INLA can be used almost as a black box to analyse latent Gaussian models [14].

Algorithm

1: Define the grid as $\lambda = (0.0005, 0.0010, . 0.01)$;
2: for $i = 1$ to 20 do;
3: calculate the vector $\mathbf{X}(i) = X(\lambda(i))$ using

ISSN: 2319-5967
ISO 9001:2008 Certified
International Journal of Engineering Science and Innovative Technology (IJESIT)
Volume 2, Issue 1, January 2013

$$\bar{X} = \lambda Q + \left(\frac{H_1^T H_1 + \ldots + H_n^T H_n}{\sigma^2}\right)^{-1} * \left(\frac{H_1^T H_1 + \ldots + H_n^T H_n}{\sigma^2}\right)$$

4: calculate the vector P *(i)* = *p*(X*(i)*|*Y)* using $p(X / Y) \propto \exp(-2K - B^T \bar{X})$
5: end for;
6: re-scale P *(i)*, by dividing each element of the vector by the sum of all elements;
7: calculate the HR image $\bar{X} = \sum_{i=1}^{20} X(i) P(i)$

Table VII. Evaluation of a reconstructed HR image considering PSNR

Test Image	Run	Adaptive Normalized Convolution	Multiframe Super Resolution	INLA MAP	INLA SR
1	1	27.20	19.44	28.88	30.45
	2	26.98	19.77	29.08	30.26
	3	27.15	18.23	29.17	30.27
	4	26.79	18.26	29.20	30.31
Average		**27.03**	**18.93**	**29.08**	**30.32**
	1	17.93	10.76	22.67	21.50
	2	17.51	11.89	21.88	21.44
	3	17.57	10.54	22.05	21.63
	4	17.51	10.53	22.04	21.64
Average		**17.63**	**10.93**	**21.99**	**21.55**

Table VII [13] shows that both INLA MAP & INLA SR algorithms obtained good results in retriving the details that were lost in the LR frames. The INLA SR method presents the best results followed by the INLA MAP method.

III.FUTURE ENHANCEMENT

From the literature it is observed that most of the techniques proposed by different researchers consumes more time. It is possible to eliminate this drawback by using the distributed environment. The algorithm can be improved for better MAE, MSE and PSNR values. More the PSNR value and lesser the MAE and MSE values, more the texture of an image can be obtained. All the algorithms can be used in wild life photography, medical imaging area. For these areas the more upscaled image will be needed. This is possible only by improving the MAE, MSE and PSNR values more than the existing values.

IV.CONCLUSION

Form the literature it is affirms that all the techniques are time consuming. The images are upscaled by using different algorithms. These algorithms work on a single processor. Many of the algorithms use MAE (Mean Absolute Error), PSNR (Peak Signal to Noise Ratio), MSE (Mean Square Error) parameters for evaluation of their results. Not much of the work has been focused on distributed environment to speed up the process of up scaling.

REFERENCES

[1] Giachetti and N. Asuni, “Real-Time Artifact-Free Image Upscaling”, IEEE Transactions On Image Processing, Vol. 20, No. 10, October 2011.

[2] J. Yang, J. Wright, T. Huang, Yi Ma, “Image Super-Resolution via Sparse Representation”.

[3] http://www.cs.utsa.edu/~qitian/seminar/Fall04/superresolution/SR_slides_xsu.pdf.

[4] M. N. Bareja, C. K. Modi, “An Effective Iterative Back Projection based Single Image Super Resolution Approach”, International Conference on Communication Systems and Network Technologies, 2012 IEEE.

[5] J. Yang, Z. Lin, S. Cohen and T. Huang, “Coupled Dictionary Training for Image Super-Resolution”, IEEE Transactions On Image Processing, Vol. 21, No. 8, August 2012.

[6] X. Gao, K. Zhang, D. Tao, and X. Li, “Image Super-Resolution With Sparse Neighbor Embedding”, IEEE Transactions On Image Processing, Vol. 21, No. 7, July 2012.

[7] F. Zhou, W. Yang, and Q. Liao, “Interpolation-Based Image Super- Resolution Using Multisurface Fitting”, IEEE Transactions On Image Processing, Vol. 21, No. 7, July 2012.

ISSN: 2319-5967
ISO 9001:2008 Certified
International Journal of Engineering Science and Innovative Technology (IJESIT)
Volume 2, Issue 1, January 2013

[8] X. Gao, K. Zhang, D. Tao, and X. Li, "Joint Learning for Single-Image Super-Resolution via a Coupled Constraint", IEEE Transactions On Image Processing, Vol. 21, No. 2, February 2012.

[9] W. Fan, J. Sun, S. Naoi, A. Minagawa, Y. Hotta, "Local Consistency Constrained Adaptive Neighbor Embedding For Text Image Super-resolution", 2012 10th IAPR International Workshop on Document Analysis Systems.

[10] S. Pelletier and J. R. Cooper stock, "Preconditioning for Edge-Preserving Image Super Resolution", IEEE Transactions On Image Processing, Vol. 21, No. 1, January 2012.

[11] J. Li and X.Peng, "Single-Frame Image Super-Resolution through Gradient Learning", IEEE International Conference on Information Science and Technology, 2012.

[12] W. Park, "Super Resolution Image Reconstruction Using Averaged Image and Regularized Deconvolution", IEEE International Conference on Robotics and Automation, 2012.

[13] M.O. Camponez, E. O. T. Salles, and M. Sarcinelli-Filho, "Super-Resolution Image Reconstruction Using Nonparametric Bayesian INLA Approximation", IEEE Transactions On Image Processing, Vol. 21, No. 8, August 2012.

[14] H. Rue, S. Martino and Nicolas Chopin, "Approximate Bayesian inference for latent Gaussian models by using integrated nested Laplace approximations", journal of Royal Statistical Society, J. R. Statist. Soc. B (2009) 71, Part 2, pp. 319–392.

[15] J. Wang, K. Liang, S, Chang and P. Chang, "Super-Resolution Image with Estimated High Frequency Compensated Algorithm", in IEEE Conf. Communication and Information Technology, 2009, pp. 1039-1042.

[16] V. B. Patel, Chintan K. Modi, C. N. Paunwala and S. Patnaik, "Hybrid Approach for Single Image Super Resolution using ISEF and IBP", in IEEE Conference on Communication System and Network Technology (CSNT), 03-05 June, 2011.